Role of liver endothelial and Kupffer cells in clearing low density lipoprotein from blood in hypercholesterolemic rabbits

Marit S. Nenseter,[1] **Ola Gudmundsen, Norbert Roos,*** **Gunhild Maelandsmo,†** **Christian A. Drevon, and Trond Berg**

Institute for Nutrition Research, University of Oslo, P.O. Box 1046, Blindern, 0316 Oslo 3, Norway; Electron Microscopic Laboratory for Biological Science,* University of Oslo, Norway; and Tumour Biology Department,† Institute for Cancer Research, Montebello, 0310 Oslo 3, Norway

Abstract The role of liver endothelial and Kupffer cells in the hepatic uptake of cholesterol-rich low density lipoprotein (LDL) was studied in rabbits fed a diet containing 2% (w/w) cholesterol for 3 weeks. ^{125}I-labeled tyramine cellobiose-labeled cholesterol-rich LDL was injected intravenously into rabbits, and parenchymal and nonparenchymal liver cells were isolated 24 h after injection. The hepatic uptake was 9 ± 3% of injected dose in cholesterol-fed rabbits 24 h after injection, as compared to 36 ± 9% in control-fed rabbits (n = 6 in each group; significant difference, $P < 0.005$). Endothelial and Kupffer cells took up 2.7 ± 0.5% and 1.2 ± 0.8% of injected dose in the hypercholesterolemic rabbits, as compared to 1.9 ± 0.8% and 0.8 ± 0.3% in control animals. The amount accounted for by the parenchymal cells was markedly reduced in the cholesterol-fed rabbits to 7.3 ± 2.7% of injected dose, as compared to 32.8 ± 7.6% in controls ($P < 0.02$). On a per cell basis, the nonparenchymal cells of cholesterol-fed rabbits took up as much LDL as the parenchymal cells (0.6 ± 0.2, 0.7 ± 0.1, and 0.6 ± 0.4% of injected dose per 10^9 parenchymal, endothelial, and Kupffer cells, respectively). This is in marked contrast to the control animals, in which parenchymal cells took up about 6 times more LDL per cell than endothelial and Kupffer cells (3.2 ± 0.9, 0.7 ± 0.3, and 0.5 ± 0.1% of injected dose per 10^9 cells). Thus, 30% of the hepatic uptake of LDL in the cholesterol-fed rabbits took place in nonparenchymal cells, as compared to 6% in controls. Consistent with these data, the concentrations of cholesteryl ester in endothelial and Kupffer cells in rabbits fed the high cholesterol diet were about twofold higher than in parenchymal cells (428 ± 74 and 508 ± 125 μg/mg protein, respectively, vs. 221 ± 24 μg/mg protein in parenchymal cells). In contrast to cells from normal rabbits, Kupffer and endothelial cells from cholesterol-fed rabbits accumulated significant amounts of Oil Red O-positive material (neutral lipids). Electron microscopic examination of these cells in situ as well as in culture revealed numerous intracellular lipid droplets. Slot blot hybridization of RNA from liver parenchymal, endothelial, and Kupffer cells showed that cholesterol feeding reduced the level of mRNA specific for the apoB,E receptor to a small and insignificant extent in all three cell types (to 70–80% of that observed in control animals). ▮ The data suggest that diet-induced hypercholesterolemia results in marked changes in the distribution of LDL in the different liver cell types, and accumulation of cholesteryl ester/lipid droplets in liver endothelial and Kupffer cells, showing that the nonparenchymal liver cells play a prominent role in removing LDL from blood in hypercholesterolemic rabbits. —Nenseter, M. S., O. Gudmundsen, N. Roos, G. Maelandsmo, C. A. Drevon, and T. Berg. Role of liver endothelial and Kupffer cells in clearing low density lipoprotein from blood in hypercholesterolemic rabbits. *J. Lipid Res.* 1992. **33:** 867–877.

Plasma clearance of low density lipoprotein (LDL) particles is predominantly mediated by the hepatic apoB,E receptor (1). Much interest has centered on the apoB,E receptor in the liver, and how it is regulated by dietary and hormonal factors (1–5). The majority of these studies has focused on the hepatic metabolism of LDL in the parenchymal liver cells or total liver. The role of the nonparenchymal liver cells in the LDL catabolism is less well described.

The nonparenchymal liver cells consist mainly of endothelial, Kupffer, and stellate (fat-storing) cells (approximately 60, 25, and 13%, respectively) (6). Although nonparenchymal cells comprise only approximately 7% of the liver protein, as much as 43% of the liver lysosomes and 26% of the total liver plasma membranes are found in these cells (7). These values are compatible with the high endocytic activities seen in the nonparenchymal cells.

The endothelial cells line the sinusoids and differ from other extrahepatic endothelial cells in several ways. They do not have a basement membrane, and display fenes-

---

Abbreviations: apo, apolipoprotein; ^{125}I-labeled TC-LDL, ^{125}I-labeled tyramine cellobiose-labeled low density lipoprotein; PC, parenchymal cells; EC, endothelial cells; KC, Kupffer cells.
[1]To whom correspondence should be addressed.

trated sieve plates that connect the sinusoidal lumen with the perisinusoidal space (space of Disse) (8–10). Thus, they form a discontinuous barrier between the lumen of the sinusoid and the parenchymal cells, which extend their microvilli into the space of Disse. The endothelial cells limit the access of particles larger than 100 nm to the space of Disse (11). The cells are very extended, and one cell often covers the whole circumference of the sinusoid. However, the cells are extremely "flat," often as thin as the diameter of a lysosome, for example. Endothelial cells are specialized to take up a number of macromolecules from the blood which are taken up only to a minor extent by other liver cells (for review, see ref. 12). This uptake is receptor-mediated, and the endothelial cell therefore displays many features attributed to receptor-mediated endocytosis, such as clathrin-coated pits, coated vesicles, early and late endosomes, and lysosomes (13, 14).

The Kupffer cells are macrophages and form the largest reservoir of macrophages in the body. They are often seen in the lumen of the sinusoid in close vicinity to the endothelial cells (8, 10). Their shape is irregular and the cytoplasm contains a variety of vesicles and many lysosomes. The outline of the nucleus is uneven.

The stellate cells have a morphology resembling that of a fibroblast and are always located in the space of Disse. Their long cytoplasmic branches often extend into the space of Disse, between parenchymal cells and endothelial lining. The most prominent feature of a stellate cell is its fat droplets, which contain a major part of the body's vitamin A content (15). The stellate cells probably take up retinol in association with retinol-binding protein; other endocytic functions have not so far been ascribed to these cells (16).

In a previous study we examined the effect of cholesterol feeding on hepatic uptake of control LDL in rabbits (17). It appeared that nonparenchymal liver cells played an important role quantitatively in the hepatic uptake of control LDL in cholesterol-fed rabbits. In the present study, LDL from cholesterol-fed rabbits was used *i*) to assess the effect of cholesterol feeding on the structure–function relationship of cholesterol-enriched LDL and on the in vivo uptake of cholesterol-rich LDL in the different liver cell types, and *ii*) to further characterize the lipid accumulation in the nonparenchymal cells in cholesterol-fed rabbits by electron microscopy.

EXPERIMENTAL PROCEDURES

Animals and diets

Male Chinchilla rabbits, 2 kg, were purchased from GMBH Versuchstierkunde und -zucht, Biberach, Germany. Some rabbits were fed Ewos Maintenance Feed containing 2% (w/w) cholesterol for 3 weeks (n = 6). Control rabbits received unsupplemented diet (n = 6).

All animals were given food and water ad libitum. Plasma cholesterol was 39 ± 8.6 mmol/l after 2 weeks of cholesterol feeding, as compared to 1.1 ± 0.2 mmol/l in control-fed rabbits, and cholesteryl ester constituted 58% and 63%, in cholesterol- and control-fed rabbits, respectively (n = 3 in each group). Plasma triacylglycerols and phospholipids were 3.8 ± 1.6 mmol/l and 9.8 ± 2.9 mmol/l, as compared to 0.9 ± 0.1 mmol/l and 1.2 ± 0.2 mmol/l in the control animals.

Cholesterol-rich LDL

After 2 weeks of cholesterol feeding, plasma from three rabbits (×2) was pooled, and two batches of cholesterol-rich LDL were isolated by sequential ultracentrifugation in the density range from 1.019 to 1.063 g/ml, and labeled with ^{125}I-labeled tyramine cellobiose (TC) as described previously (17). The final preparations were dialyzed against 0.15 M NaCl, 20 mM sodium phosphate, and 1 mM EDTA (PBS), pH 7.4. More than 98% of the radioactivity in the labeled lipoproteins was precipitated by 10% (w/v) TCA. The final specific activities of the two batches of ^{125}I-labeled TC-LDL were 50 and 355 cpm/ng of protein.

Metabolic studies

^{125}I-labeled TC-LDL was injected into the marginal ear vein. Blood samples (100 μl) were drawn from the vein of the opposite ear at indicated time points, and radioactivity was quantified using a Kontron Automatic Gamma Counter MB252. Fractional catabolic rate was calculated from plasma tracer data by using double exponential decay equation (18). The absolute catabolic rate was calculated by multiplying the fractional catabolic rate (pools per day) by the apoLDL pool size. Plasma volume was assumed to be 3.28% of body weight (19). After 24 h the rabbits were anesthetized by intraperitoneal injection of Dormicum (Roche), 0.5 ml/kg, and 5 min later by intramuscular injection of Hypnorm (Janssen), 0.4 ml/kg. All rabbits were killed at the same time of the day (9–10 AM). Isolated liver cells were prepared by collagenase perfusion of the liver, as described previously (17). At the end of preperfusion, a lobe was removed and washed in ice-cold PBS before total radioactivity was measured. One part of the lobe was subjected to glutaraldehyde fixation and used for electron microscopy studies (see details below). After collagenase perfusion, parenchymal and nonparenchymal cells were separated by centrifugal elutriation using a Beckman JE-6 rotor. Hepatocytes were eluted at 1200 rpm at a flow rate of 25–55 ml/min. Nonparenchymal cells were eluted at 1500 rpm at a flow rate of 20 ml/min. Pure endothelial and Kupffer cells were prepared by a selective attachment culturing method, as described before (17). The liver weight was calculated as 3.47% of body weight (determined in a separate group of control rabbits; SD = ±0.38%; n = 4).

Lipoprotein particle size

LDL particle size was determined by dynamic light scattering Photon Correlation Spectroscopy (20), and by negative staining electron microscopy (21). LDL preparations used for Photon Correlation Spectroscopy were diluted in PBS, and filtered through 0.45-μm filter just before use (Sterivex, Millipore). A Spectra Physics model 2020 Argon Ion Laser was used as light source. The detected scattering intensity was monitored. A reference specimen containing latex particles with a diameter of 54.5 nm was used to adjust the optical alignment for each experiment.

RNA analysis

RNA was isolated from purified cells by a LiCl/urea procedure, essentially as described previously (22–24). Five μg of total RNA was size-separated by electrophoresis on 1% agarose/formaldehyde gels buffered with NaH_2PO_4, and blotted onto nylon membranes (Bio-Rad Zetaprobe) (23). Slot blots were made as described before (24). After baking at 80°C for 2 h, the blots were UV-crosslinked and hybridized as described by Church and Gilbert (25). ApoB,E receptor mRNA was detected by using the pLDLR-11 plasmid generously provided by Drs. D. W. Russell, J. L. Goldstein, and M. S. Brown of the University of Texas, Health Science Center, Dallas, Texas (26). The probe was prepared from a 2.5 kb SmaI fragment by randomly primed extension (27). Standardization of RNA amounts was done by hybridization of the filters to a kinase-labeled oligonucleotide (22 bases) specific for 28S rRNA (23). For quantitation of signals on the blots, the autoradiograms were scanned densitometrically on a Molecular Dynamics Computing Densitometer.

Oil Red O staining

Liver parenchymal, endothelial, and Kupffer cells from control- and cholesterol-fed rabbits were stained with Oil Red O for overall localization of lipids. Cultured cells were subjected to fixation in 2.5% glutaraldehyde in PBS, pH 7.4, washed, and stained in freshly filtered Oil Red O in 60% isopropanol for 10 min (28). Cells were examined by phase-contrast microscopy.

Electron microscopy

Liver lobes from control- and cholesterol-fed rabbits were examined by electron microscopy for the accumulation of lipid droplets. After preperfusion of the liver with Ca^{2+}-free buffer, small pieces of the liver were removed, put in buffer containing 2.5% glutaraldehyde, and immediately cut into small blocks of about 1 mm³. After glutaraldehyde fixation for 48 h at 4°C, the fixation buffer was replaced by a 0.1 M cacodylic acid buffer (pH 7.4) and the tissue pieces were washed twice for 10 min at 4°C. The samples were postfixed with 4% OsO_4 in cacodylic

acid buffer (pH 7.4) for 2 h at 0°C and washed twice for 20 min with the same buffer without OsO_4. After rinsing, the samples were dehydrated in an increasing gradient of ethanol (70%, 90%, 96%, and 100%) and embedded in Spurr resin. After polymerization of the resin at 70°C for 24 h and at 60°C for 72 h, 50-nm sections were cut on an LKB III microtome using glass knives. The sections were placed on formvar/carbon-coated 75-mesh copper grids and stained for 2 min with a saturated uranyl acetate solution in 50% ethanol and 2 min in 0.2% lead citrate solution in 0.1 N NaOH.

Parenchymal, endothelial, and Kupffer cells prepared by the selective attachment method (17, 20), were grown in RPMI 1640 on Falcon 3006 optical dishes (60 × 15 mm) and fixed, postfixed, and dehydrated as described above for liver lobes. A mixture of Spurr resin and 100% ethanol at ratio of 1:2 was added for 15 min, replaced by a mixture of 1:1 for another 15 min, and finally by 100% Spurr resin. The dishes were covered with 2–3 mm Spurr resin and beam capsules with the tip cut off were placed on the dishes. After polymerization of the resin at 60°C for 20 h, the capsules were filled with resin and polymerized at 60°C for 24 h. The beam capsules were broken lose from the petri dish and much of the petri dish material was trimmed away. Sections were cut, placed on copper grids, and stained as described above. The sections were examined using a JEOL 100C and JEOL 100CX transmission electron microscope and an accelerating voltage of 80 kV.

Chemical assays

Cholesterol and phospholipids in plasma and LDL were determined enzymatically by kits from Bio Merieux, Marcy-l'Etoile, France; triacylglycerol was determined enzymatically by Nycotest kit, Nycomed A/S, Oslo, Norway. Free and esterified cholesterol in cultured cells were measured by gas–liquid chromatography. Stigmasterol was added to the cells, and they were extracted according to Folch, Lees, and Sloane Stanley (29). Two μl of lipids redissolved in n-hexane was subjected to gas–liquid chromatography. Cholesteryl ester was determined as the difference between free cholesterol measured before and after saponification. A Shimadzu, equipped with a 6 ft, 2 mM I.D. column was used at 295°C with argon as carrier gas (30). Protein concentration was determined by the method of Lowry et al. (31) using bovine serum albumin as standard. SDS polyacrylamide gradient gel electrophoresis (5–20%) of lipoprotein preparations was performed according to Laemmli (32). Autoradiograms were scanned in a Beckman DU Spectrophotometer.

Statistical analysis

All results are presented as means ± standard deviations (SD). Mann-Whitney two-sample test or Student's

t-test was used for calculation of statistic significance of differences between groups.

RESULTS

Composition and particle size of cholesterol-rich LDL

The LDL from pooled plasma of rabbits (n = 3) fed 2% (w/w) cholesterol for 2 weeks consisted of 61.1% cholesterol, 3.0% triacylglycerols, 13.2% phospholipids, and 22.7% protein (**Table 1**). Cholesteryl esters accounted for 63% of the total cholesterol content. The composition of control LDL used in previous studies is included in Table 1 for comparative purposes. The LDL fraction from cholesterol-fed rabbits contained apoE in addition to apoB-100, and 16% of the radioactivity was present in the apoE moiety of the labeled LDL particles. The ratio (w/w) of cholesterol to protein was fourfold higher in cholesterol-rich LDL than in control LDL (2.7 vs. 0.7). The particle size of LDL from cholesterol-fed rabbits, measured by light scattering, was significantly larger than control LDL (390 ± 60 Å in diameter vs. 290 ± 80 Å). The LDL fractions were also negatively stained and examined in the electron microscope to assess particle size and structure. LDL particles from cholesterol-fed rabbits were slightly irregular in shape and measured 240 ± 38 Å in diameter (n = 16), whereas LDL particles from control animals had an apparent diameter of 190 ± 33 Å (n = 20), and were spherical in shape. These apparent sizes of the particles are smaller than the values obtained from laser scattering measurements. This could be due to the fact that the particles were in solution for laser scattering measurements and therefore fully hydrated, whereas negatively stained particles may have shrunk during the staining and drying process.

Fig. 1. Plasma clearance curves of ^{125}I-labeled TC-cholesterol-rich LDL intravenously injected into control- and cholesterol-fed rabbits. Data are expressed as % of the amount of radioactivity present in plasma 5 min after injection, and show means ± SD of six rabbits in each group.

Plasma clearance of cholesterol-rich LDL

Cholesterol-rich LDL was removed from plasma at a considerably slower rate in cholesterol-fed rabbits than in the control rabbits (n = 6 in each group) (**Fig. 1**). Fractional catabolic rate was reduced to about 30% of that observed in control animals (1.18 ± 0.12 vs. 0.38 ± 0.13 pools/24 h), whereas absolute catabolic rate was >fourfold higher in the hypercholesterolemic rabbits (31.6 ± 8.1 vs. 6.7 ± 0.7 mg/kg/24 h). The time an average molecule of cholesterol-rich LDL spent in the plasma compartment during a single transit (mean transit time) was 42.5 ± 10.4 h in the hypercholesterolemic rabbits, as compared to 14.2 ± 1.5 h in the controls.

Hepatic uptake of cholesterol-rich LDL

The proportion of injected radiolabeled cholesterol-rich LDL taken up by the liver was greatly reduced in the cholesterol-fed rabbits. Twenty-four hours after injection the hepatic uptake was 9 ± 3% of injected dose in cholesterol-fed rabbits, as compared to 36 ± 9% in control-fed rabbits (n = 6 in each group; significant difference, P < 0.005).

Analysis of labeled LDL that accumulated in the various types of liver cells revealed that the reduced relative hepatic uptake in cholesterol-fed animals could be accounted for by reduced uptake in parenchymal cells. The endothelial cells and Kupffer cells, on the other hand, tended to take up more cholesterol-rich LDL after cholesterol feeding (**Fig. 2A**), and it could be calculated that the

TABLE 1. Composition of LDL particles from control- and cholesterol-fed rabbits

	Control LDL[a]		Cholesterol-rich LDL[b]	
	mg/mg protein	%	mg/mg protein	%
FC	0.33 ± 0.01	10.9 ± 1.1	0.99	22.6
CE	0.41 ± 0.14	13.3 ± 0.7	1.69	38.5
TG	0.49 ± 0.35	14.3 ± 8.5	0.13	3.0
PL	0.84 ± 0.34	26.6 ± 3.7	0.58	13.2
Protein	1.00	34.9 ± 11.7	1.00	22.7
Total	3.07 ± 0.89		4.39	

FC, free cholesterol; CE, cholesteryl ester; TG, triacylglycerol; PL, phospholipid

[a]Control LDL: Results are means ± SD; n = 3. Data are included for comparison.

[b]Cholesterol-rich LDL was isolated from pooled rabbit plasma (n = 3). Rabbits were fed cholesterol (2% w/w) for 2 weeks.
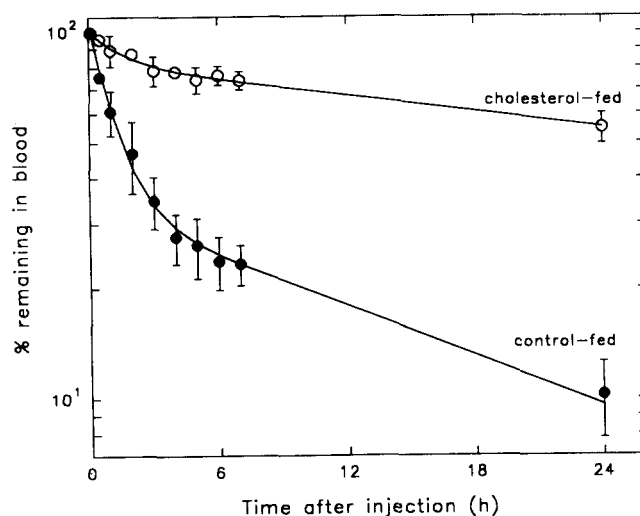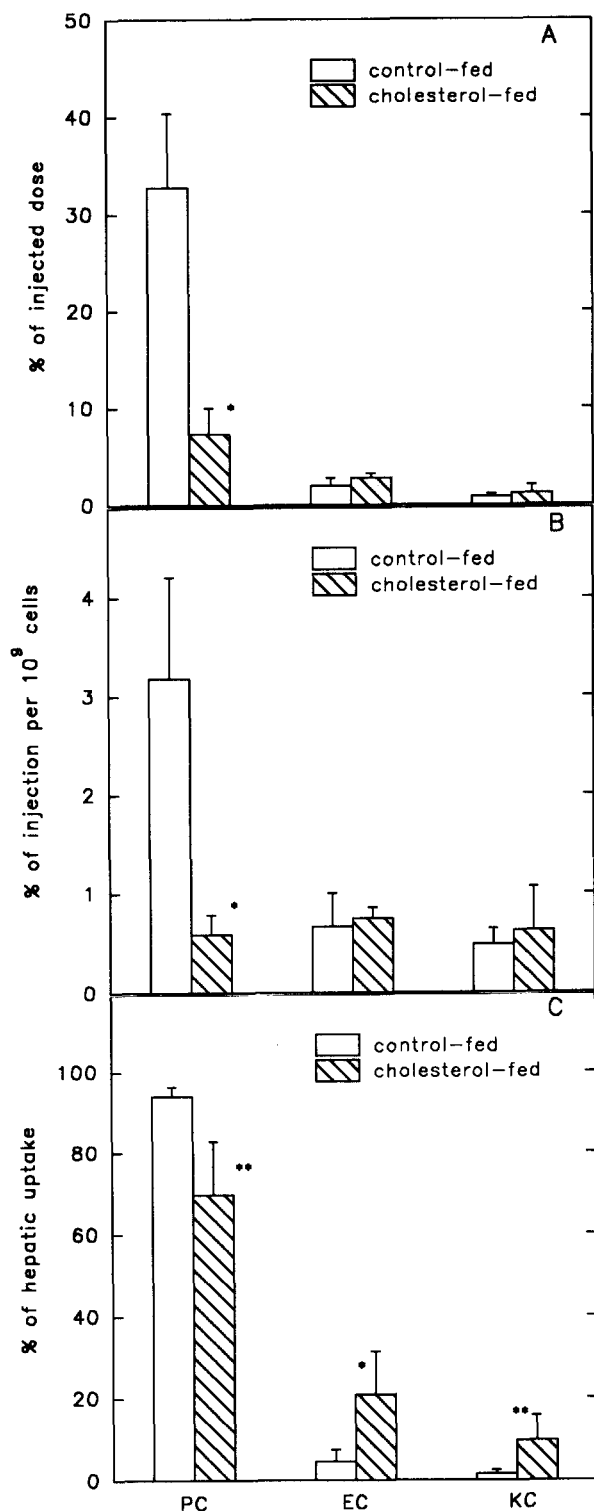
Fig. 2. Uptake of intravenously injected ^{125}I-labeled TC-cholesterol-rich LDL in liver parenchymal (PC), endothelial (EC), and Kupffer cells (KC) in control- and cholesterol-fed rabbits. The various cell types were isolated 24 h after injection. Results are expressed as means ± SD of % of injected dose taken up in the liver (panel A); % of injected dose per 10^9 cells (panel B); % of hepatic uptake (panel C); n = 6 in each group; *, $P < 0.02$ vs. control; **, $P < 0.005$ vs. control. The recovery of radioactive LDL in the cells was 99% and 124% in control- and cholesterol-fed rabbits, respectively, of that in the liver from which the cells were derived.

nonparenchymal cells took up as much LDL per cell as the parenchymal cells (0.6 ± 0.2, 0.7 ± 0.1, and 0.6 ± 0.4% of injected dose per 10^9 parenchymal, endothelial, and Kupffer cells, respectively) (Fig. 2B). This is in marked contrast to the control animals in which parenchymal cells took up about 6 times more LDL per cell than endothelial and Kupffer cells (3.2 ± 0.9, 0.7 ± 0.3, and 0.5 ± 0.1% of injected dose per 10^9 cells) (Fig. 2B). The prominent role of the nonparenchymal cells in taking up LDL in cholesterol-fed rabbits is also seen when the uptake in parenchymal and nonparenchymal cells is calculated as per cent of total hepatic uptake (Fig. 2C). Thus, 30% of the hepatic uptake of LDL in the cholesterol-fed rabbits took place in nonparenchymal cells, as compared to 6% in controls.

The changes in the composition and size of the LDL particle induced by cholesterol feeding did not markedly affect its distribution to the parenchymal and nonparenchymal liver cells. **Table 2** shows that the cellular distribution of control LDL (17) and cholesterol-rich LDL is similar in both control and cholesterol-fed rabbits. The Kupffer cells may possibly take up more cholesterol-rich LDL than control LDL in the cholesterol-fed rabbits.

ApoB,E receptor-specific mRNA

Slot blot hybridization of RNA from liver cells showed that the amounts of apoB,E receptor-specific mRNA in parenchymal, endothelial, and Kupffer cells in cholesterol-fed rabbits were 67 ± 14, 77 ± 13, and 72 ± 35%, respectively, of the amount in control animals (n = 4 and n = 3 for control- and cholesterol-fed rabbits, respectively; $P > 0.05$ for all three cell types) (**Fig. 3**). Thus, the level of apoB,E receptor-specific mRNA was not significantly altered in the different liver cell types by dietary cholesterol supplement. Northern blot analysis confirmed the slot blot-based quantitations of mRNA levels in parenchymal and endothelial cells. Reliable results from Northern blots of Kupffer cells were not achieved due to smearing from degradation, a problem that was avoided when using slot blot.

Hepatic cholesteryl ester accumulation

After 3 weeks of cholesterol feeding, relatively small changes occurred in the level of free cholesterol in the parenchymal and endothelial cells, whereas a significant increase in the amount of free cholesterol was measured in Kupffer cells ($P < 0.002$; **Table 3**). In marked contrast, a dramatic increase in the content of cholesteryl ester was observed, accounting for approximately 80% of the total cholesterol content in all three cell types. It should be noted that the concentration of cholesteryl ester in endothelial and Kupffer cells was approximately two-fold higher than in parenchymal cells (428 ± 74 and 508 ± 125 μg/mg protein, respectively, vs. 221 ± 24 μg/mg protein in parenchymal cells; $P < 0.05$ vs. paren-

TABLE 2. Distribution of LDL in the liver parenchymal (PC), endothelial (EC), and Kupffer cells (KC) 24 h after injection

	Control LDL			Cholesterol-rich LDL		
Rabbits	PC	EC	KC	PC	EC	KC
	% of total hepatic uptake					
Control-fed	92.4 ± 4.6	4.0 ± 2.9	3.6 ± 2.1	93.9 ± 2.4	4.5 ± 2.9	1.6 ± 0.9
Cholesterol-fed	74.0 ± 9.8	21.3 ± 10.6	4.7 ± 1.5	69.6 ± 13.2**	20.8 ± 10.5*	9.6 ± 6.1**

Results are mean ± SD; n = 4 and n = 6 for control and cholesterol-rich LDL, respectively. Results concerning control LDL are included for comparison (ref. 17). *$P < 0.02$; **$P < 0.005$ vs. control-fed rabbits.

chymal cells). These results are consistent with the increased uptake of cholesterol-rich LDL observed in endothelial and Kupffer cells in these rabbits.

Morphology

Examination of the cells by light microscopy demonstrated large lipid droplets in all three cell types from cholesterol-fed rabbits. Staining neutral lipids in the cultured nonparenchymal cells with Oil Red O revealed that Kupffer and endothelial cells from cholesterol-fed rabbits accumulated significant amounts of Oil Red O-positive material (**Fig. 4C and D**), in contrast to cells from normal rabbits, which did not stain with Oil Red O (Fig. 4A and B). Thus, all the endothelial cells accumulated lipid droplets as compared to 72% of the Kupffer cells (115 cells counted). The presence of lipid droplets in the nonparenchymal liver cells from the cholesterol-fed rabbits was also examined by transmission electron microscopy. The arrangement of the rabbit liver cells as seen in ultrathin, post-stained sections of resin-embedded rabbit liver of control animals corresponded to the description given in the introductory section (**Fig. 5A**). Very few fat droplets were seen in cells from control animals. The in situ arrangement of the cells was not changed in cholesterol-fed rabbits (Fig. 5B). However, the endothelial cells showed a large number of intracellular lipid droplets. Some Kupffer

cells also displayed numerous lipid droplets. The Kupffer cell (panel B) occluding the lumen of the sinusoid is not a common feature, but can be observed occasionally. The average diameter of lipid droplets in nonparenchymal cells was only about 20% of that observed in parenchymal cells.

The cultured Kupffer cells contained dense bodies, very irregularly shaped nuclei, and some long and thin cytoplasmic extensions (**Fig. 6A**). In contrast, the endothelial cells grown on dishes seemed "collapsed" (Fig. 6B). The arrangement of the thin and very long cytoplasmic extensions with the sieve plates containing the fenestrations are now reduced to a curl-like structure. Cultured cells from cholesterol-fed rabbits appeared similar to control cells except that endothelial cells contained numerous intracellular lipid droplets and long rod-shaped lysosomes probably consisting mainly of cholesterol crystals (Fig. 6D). Consistent with the Oil Red O staining of the cells (Fig. 4), most Kupffer cells contained lipid droplets, but they were less abundant than in the endothelial cells (Fig. 6C).

DISCUSSION

The results of the present study indicate that the nonparenchymal liver cells assume a prominent role in clearing LDL from blood in hypercholesterolemic rabbits.
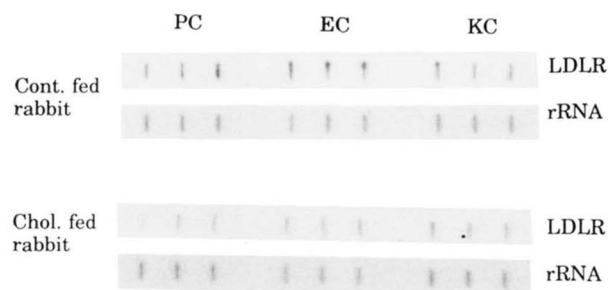

Fig. 3. Typical expression pattern of apoB,E receptor mRNA in rabbit liver cells. Slot blot of RNA from liver parenchymal (PC), endothelial (EC), and Kupffer cells (KC) from control- and cholesterol-fed rabbits. Three parallels from each sample were hybridized to the apoB,E receptor probe and subsequently to a probe specific for 28S rRNA. Results are representative for four control-fed rabbits and three cholesterol-fed rabbits. The data were normalized relative to the amount of rRNA and expressed as percent of control values.

TABLE 3. Cellular content of free and esterified cholesterol in parenchymal (PC), endothelial (EC), and Kupffer cells (KC) of control and cholesterol-fed rabbits

Rabbits	Total Cholesterol	Free Cholesterol	Cholesteryl Ester
	μg/mg protein		
Control-fed			
PC	10 ± 3	11 ± 3	n.d.
EC	148 ± 17	153 ± 26	n.d.
KC	65 ± 18	31 ± 19	34 ± 8
Cholesterol-fed			
PC	264 ± 37**	43 ± 24	221 ± 24
EC	522 ± 73*	94 ± 5	428 ± 74
KC	690 ± 114*	182 ± 13***	508 ± 126*

Rabbits were cholesterol-fed (2% w/w) for 3 weeks. Results are mean ± SD; n = 3 in each group. n.d., not detectable. *, $P < 0.05$; **, $P < 0.01$, ***, $P < 0.002$ vs. control.
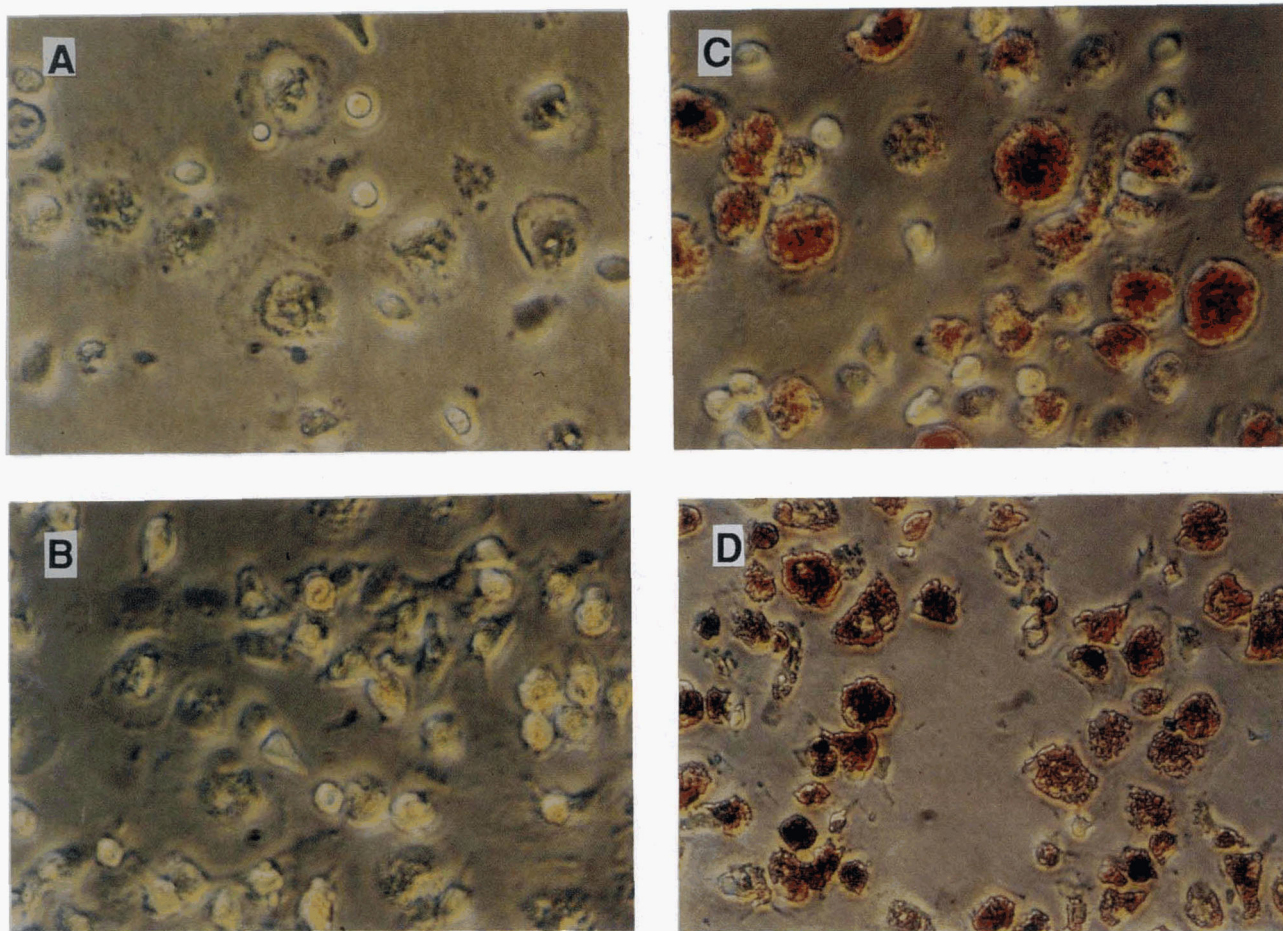
Fig. 4. Kupffer cells (KC) and endothelial cells (EC) from control-fed (panels A and B) and cholesterol-fed (panels C and D) rabbits stained with Oil Red O. KC were cultured on dishes pretreated with bovine serum albumin and glutaraldehyde, and thoroughly washed with PBS before seeding of cells. EC (panels B and D) were seeded on fibronectin-coated dishes.

Thus, these cells account for 30% of the hepatic uptake in cholesterol-fed rabbits as compared to 6% in controls. Both Kupffer and endothelial cells contribute to the increased uptake by the nonparenchymal cells. However, the endothelial cells, which are more numerous, take up more than twice as much LDL as the Kupffer cells.

The composition and size of the LDL particle is modified by the cholesterol feeding, but this is not the reason for the increased uptake by the nonparenchymal cells. The cellular distribution pattern of control LDL is similar to that of cholesterol-rich LDL in cholesterol-fed as well as control rabbits. This suggests an additional modification of cholesterol-rich LDL, which also occurs for control LDL injected into hypercholesterolemic rabbits. In other words, control LDL may be modified during the 24 h residence time in cholesterol-fed rabbits.

The prominent role assumed by the liver endothelial and Kupffer cells in clearing LDL in the hypercholesterolemic rabbit is supported by the striking accumulation of cholesteryl ester in these cells. This was also visualized as

lipid droplets by electron microscopy of endothelial and Kupffer cells in situ and in culture. The increased uptake of LDL in nonparenchymal cells is even more dramatic when expressed in absolute terms, since the plasma pool of LDL is at least 15 times higher in the hypercholesterolemic rabbits than in control animals. The increased uptake is probably accounted for by scavenger receptors present in both Kupffer and endothelial cells. The prolonged mean transit time for LDL in the plasma of cholesterol-fed rabbits (see above) increases the likelihood of the particle to be modified such that it becomes a ligand for the scavenger receptor. It has been shown that lipid peroxidation in plasma and liver may be induced by cholesterol feeding of experimental animals (33, 34). Cholesterol feeding may therefore contribute to oxidative modification of LDL to a form recognized by the scavenger receptors in endothelial and Kupffer cells, transforming these cells into lipid-loaded cells with a foam cell-like morphology. In fact, our preliminary data suggest that cholesterol-rich LDL, isolated from rabbits after 2 weeks
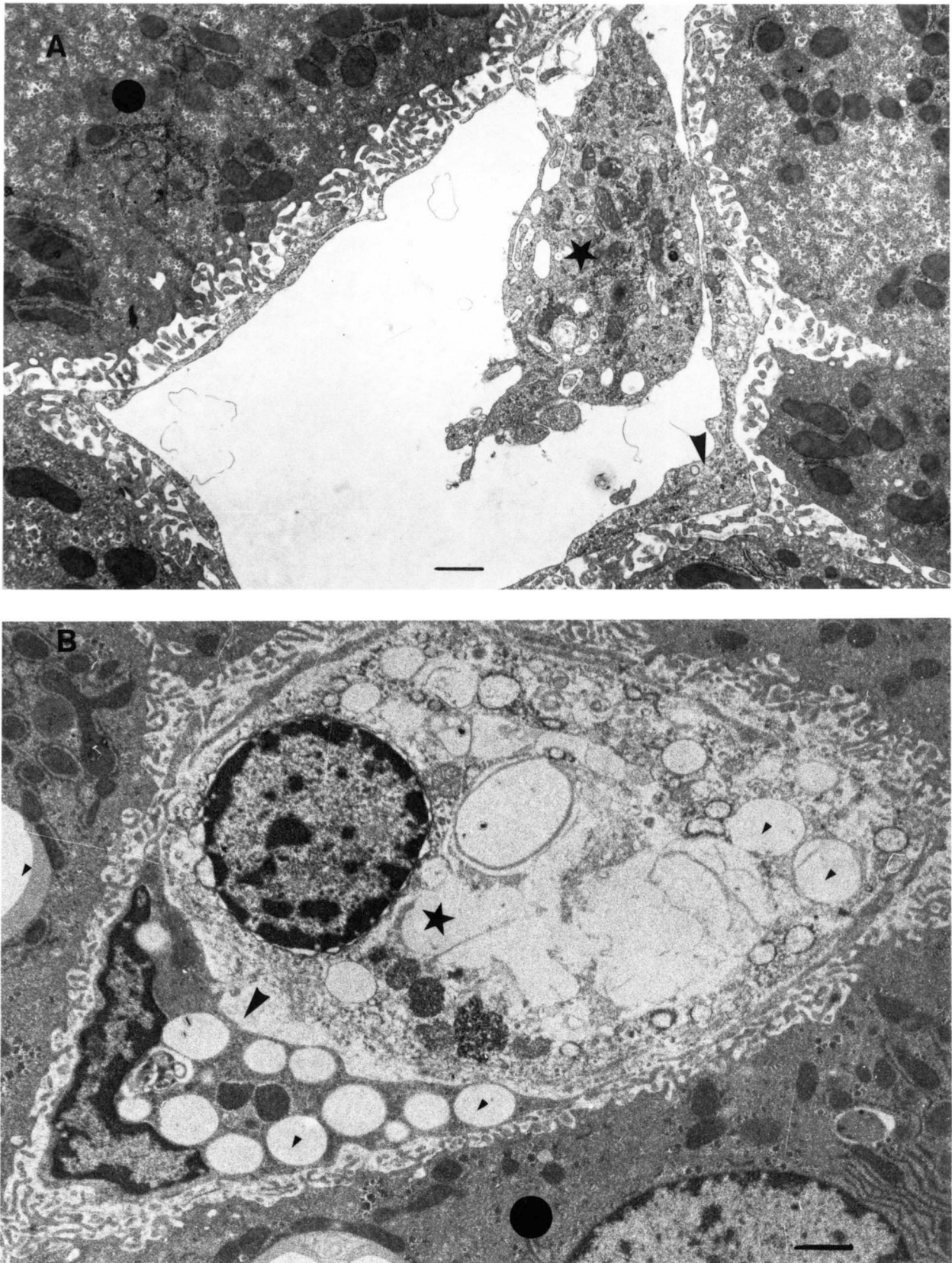
Fig. 5. Appearance of various liver cells in control (panel A) and cholesterol-fed (panel B) rabbits in situ. The specimen preparation for electron microscopy was performed as described in the Experimental section. Black dots label parenchymal cells, stars label Kupffer cells, and large arrowheads label the endothelial lining. Small arrowheads indicate lipid droplets. Bar represents 1 μm.
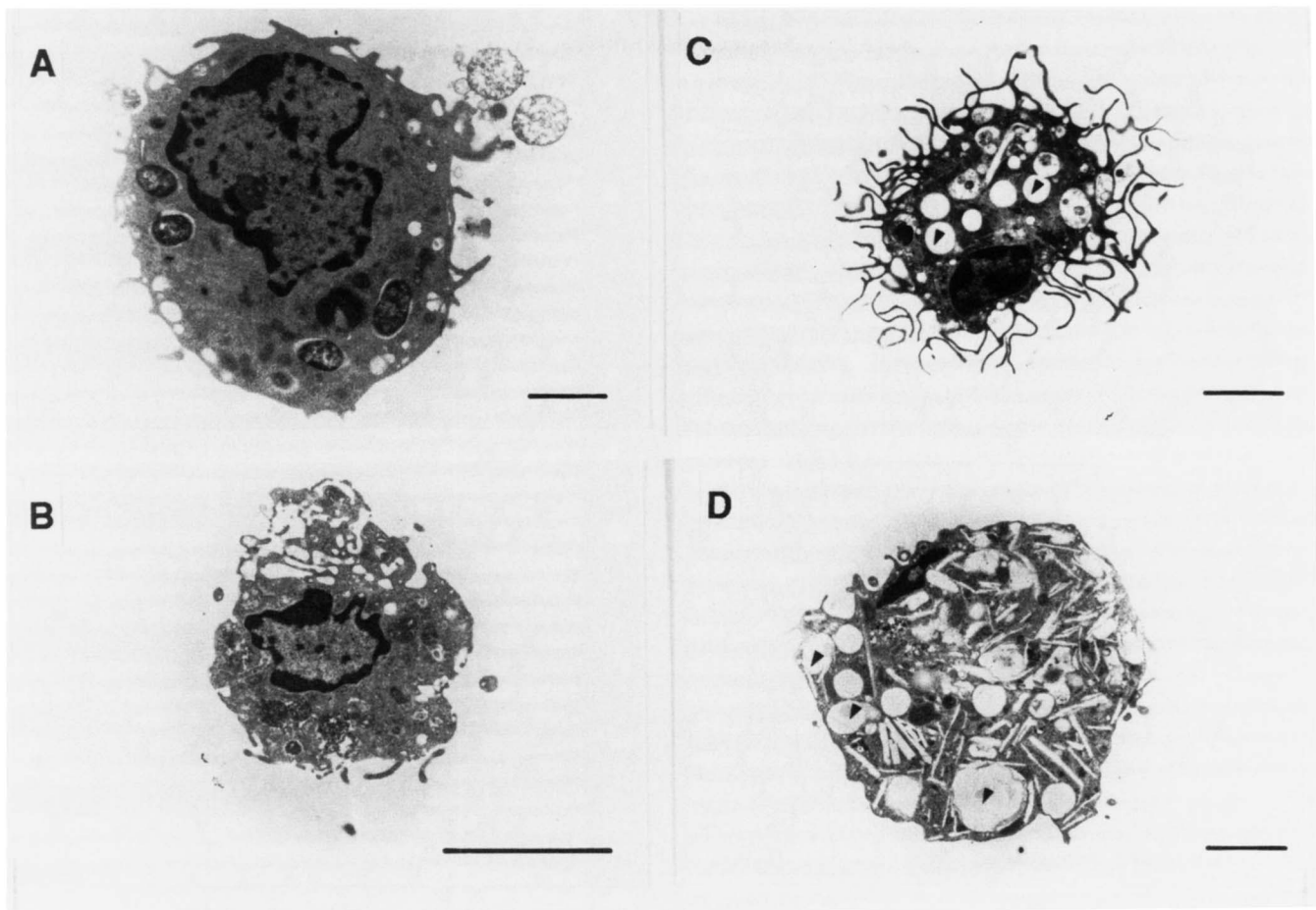
Fig. 6. Appearance of nonparenchymal liver cells of control-fed (panels A and B) and cholesterol-fed (panels C and D) rabbits. The cells were grown on optical dishes and prepared for electron microscopy as described in the experimental section. Panels A and C depict Kupffer cells and panels B and D endothelial cells from control and cholesterol-fed rabbits, respectively. Small arrowheads indicate lipid droplets. Bar represents 2 μm.

of cholesterol supplementation, is much more susceptible to copper-catalyzed lipid peroxidation than control LDL (Nenseter, M. S., C. A. Drevon, T. Berg, and O. Gudmundsen, unpublished results).

It has been shown that a hepatic scavenger receptor that mediates uptake of acetylated LDL is present mainly in liver endothelial cells (35, 36). The present results suggest that endothelial and Kupffer cells are equally important in terms of uptake per cell. This is compatible with a recent report suggesting that oxidized LDL is recognized by scavenger receptors on both Kupffer and endothelial cells (37). Our data show that nonparenchymal cells in cholesterol-fed rabbits take up control LDL to a similar extent as cholesterol-rich LDL (Table 1). The Kupffer cells, however, may be more effective in the uptake of cholesterol-rich LDL. This is in agreement with the notion that cholesterol-rich LDL is more susceptible to oxidation.

The fraction of injected dose of LDL taken up by the parenchymal cells in the cholesterol-fed rabbits was markedly reduced as compared to control animals. How-

ever, taking into account the increased plasma pool-size of LDL, the absolute amount of LDL taken up by parenchymal cells is significantly increased in the cholesterol-fed rabbits, as emphasized by the enhanced absolute catabolic rate measured in these animals. Furthermore, this is also supported by the increased amount of cholesteryl ester in the parenchymal, endothelial, and Kupffer cells, and the lipid droplets seen in these cells by electron microscopy. Taken together, our data suggest that the flux of LDL into the liver is increased in the cholesterol-fed rabbits, raising the question by which uptake mechanism(s) this occurs. In a previous study (17) we showed that native and methylated LDL were cleared from plasma at similar rates in the hypercholesterolemic rabbits, suggesting that LDL was removed by an apoB,E receptor-independent pathway. However, the data suggested that approximately 60% of the uptake of LDL in parenchymal cells was apoB,E receptor-dependent in these animals. In the present study we observed an insignificant reduction in the level of mRNA for the apoB,E receptor in cholesterol-fed animals. This is in agreement with the observa-

tion that the hepatic apoB,E receptor mRNA is relatively insensitive to metabolic perturbations compared to apoB,E receptor activity, suggesting that a post-transcriptional regulation may be operative in the liver. In spite of reduced receptor activity, LDL may be more efficiently taken up by the apoB,E receptor in the hypercholesterolemic rabbits, since LDL contains apoE in these animals. In addition, the increased amount of hepatic cholesterol may be accounted for by alternative uptake mechanisms. As discussed above, our data suggest that LDL is taken up by the scavenger receptor in endothelial and Kupffer cells. Scavenger receptor activity has also been reported to be present in liver parenchymal cells in the rat (36, 37). This receptor is probably not down-regulated by intracellular accumulation of cholesteryl ester, and therefore, it is possible that the scavenger receptor may be responsible for part of the uptake of LDL in parenchymal cells in the hypercholesterolemic rabbits.

Taken together, our data suggest that i) the larger particle size and increased cholesterol to protein ratio of LDL caused by cholesterol feeding did not in itself affect the hepatic uptake of LDL. Rather, cholesterol feeding probably modified LDL to a ligand recognized by the scavenger receptor. Thus, marked differences in the uptake of LDL in different types of liver cells from control and cholesterol-fed rabbits were observed, regardless of the source of LDL. ii) Diet-induced hypercholesterolemia results in accumulation of cholesteryl ester/lipid droplets in liver endothelial and Kupffer cells. Thus, the nonparenchymal liver cells probably play a prominent role in removing LDL from blood in hypercholesterolemic rabbits. 🔳

REFERENCES

1. Brown, M. S., and J. L. Goldstein. 1986. A receptor-mediated pathway for cholesterol homeostasis. *Science.* **232:** 34–47.
2. Spady, D. K., and J. M. Dietschy. 1985. Dietary saturated triacylglycerols suppress hepatic low density lipoprotein receptor activity in the hamster. *Proc. Natl. Acad. Sci. USA.* **82:** 4526–4530.
3. Spady, D. K., and J. M. Dietschy. 1988. Interaction of dietary cholesterol and triglycerides in the regulation of hepatic low density lipoprotein transport in the hamster. *J. Clin. Invest.* **81:** 300–309.
4. Fox, J. C., H. C. McGill, Jr., K. D. Carey, and G. S. Getz. 1987. In vivo regulation of hepatic LDL receptor mRNA in the baboon. *J. Biol. Chem.* **262:** 7014–7020.
5. Ma, P. T. S., T. Yamamoto, J. L. Goldstein, and M. S. Brown. 1986. Increased mRNA for low density lipoprotein receptor in livers of rabbits treated with 17α-ethinyl estradiol. *Proc. Natl. Acad. Sci. USA.* **83:** 792–796.
6. Knook, D. L., and E. C. Sleyster. 1976. Separation of Kupffer and endothelial cells of rat liver by centrifugal elutriation. *Exp. Cell Res.* **99:** 444–449.
7. Blouin, A., R. P. Bolender, and E. R. Weibel. 1977. Distribution of organelles and membranes between hepatocytes and nonhepatocytes in the rat liver parenchyma. *J. Cell Biol.* **72:** 441–455.
8. Aterman, K. 1963. *In:* The Liver: Morphology, Biochemistry, Physiology. C. Rouiller, editor. Academic Press, New York. **Vol. 1:** 61–136.
9. Wisse, E. 1970. An electron microscopic study of the fenestrated endothelial lining of rat liver sinusoids. *J. Ultrastruct. Res.* **31:** 125–150.
10. Wisse, E. 1972. An ultrastructural characterization of the endothelial cell in the rat liver sinusoid under normal and various experimental conditions, as a contribution to the distinction between endothelial and Kupffer cells. *J. Ultrastruct. Res.* **38:** 528–562.
11. Naito, M., and E. Wisse. 1978. Filtration effect of endothelial fenestrations on chylomicron transport in the neonatal rat liver. *Cell Tissue Res.* **190:** 371–382.
12. Smedsrød, B., H. Pertoft, S. Gustafson, and T. C. Laurent. 1990. Scavenger functions of the liver endothelial cell. *Biochem. J.* **266:** 313–327.
13. Stang, E., G. M. Kindberg, T. Berg, and N. Roos. 1990. Endocytosis of mannose-terminated glycoproteins in rat liver endothelial cells. *Eur. J. Cell Biol.* **52:** 67–76.
14. Seydel, W., E. Stang, N. Roos, and J. Krause. 1991. Endocytosis of the recombinant tissue plasminogen activator alteplase by hepatic endothelial cells. *Drug Res.* **41:** 182–186.
15. Wake, K. 1971. Sternzellen in the liver: perisinusoidal cells with special reference to storage of vitamin A. *Am. J. Anat.* **132:** 429–461.
16. Gjøen, T., T. Bjerkelund, H. K. Blomhoff, K. R., Norum, T. Berg, and R. Blomhoff. 1987. Liver takes up retinol-binding protein from plasma. *J. Biol. Chem.* **262:** 10926–10930.
17. Nenseter, M. S., R. Blomhoff, C. A. Drevon, G. M. Kindberg, K. R. Norum, and T. Berg. 1988. Uptake of LDL in parenchymal and nonparenchymal rabbit liver cells in vivo. *Biochem. J.* **254:** 443–448.
18. Matthews, C. M. E. 1957. The theory of tracer experiments with ¹³¹I-labeled plasma proteins. *Phys. Med. Biol.* **2:** 36–53.
19. Ross, A. C., and D. B. Zilversmit. 1977. Chylomicron remnant cholesteryl esters as the major constituent of very low density lipoproteins in plasma of cholesterol-fed rabbits. *J. Lipid Res.* **18:** 169–181.
20. Berne, B. J., and R. Pecora. 1976. Dynamic Light Scattering. John Wiley & Sons Inc., New York.
21. Collins, J. J., and M. C. Phillips. 1982. The stability and structure of cholesterol-rich codispersions of cholesterol and phosphatidylcholine. *J. Lipid Res.* **23:** 291–298.
22. Birnboim, H. C. 1988. Rapid extraction of high molecular weight RNA from cultured cells and granulocytes for Northern analysis. *Nucleic Acids Res.* **16:** 1487–1497.
23. Maniatis, T., E. F. Fritsch, and J. Sambrook. 1989. Molecular Cloning: A Laboratory Manual. Cold Spring Harbor Laboratory, Cold Spring Harbor, New York.

24. Nenseter, M. S., O. Myklebost, R. Blomhoff, C. A. Drevon, A. Nilsson, K. R. Norum, and T. Berg. 1989. Low density lipoprotein receptors in different rabbit liver cells. *Biochem. J.* **261:** 587–593.

25. Church, G. M., and W. Gilbert. 1984. Genomic sequencing. *Proc. Natl. Acad. Sci. USA.* **81:** 1991–1995.

26. Yamamoto, T., R. W. Bishop, M. S. Brown, J. L. Goldstein, and D. W. Russell. 1986. Deletion of cysteine-rich region of LDL receptor impedes transport to cell surface in WHHL rabbit. *Science.* **232:** 1230–1237.

27. Feinberg, A. P., and B. Vogelstein. 1983. A technique for labeling DNA restriction fragments to high specific activity. *Anal. Biochem.* **132:** 6–13.

28. Pearse, A. G. E. 1960. Histochemistry, Theoretical and Applied. J & A Churchill Ltd., London. 854.

29. Folch, J., M. Lees, and G. H. Sloane Stanley. 1957. A simple method for the isolation and purification of total lipids from animal tissues. *J. Biol. Chem.* **226:** 497–509.

30. Rustan, A. C., J. Ø. Nossen, H. Osmundsen, and C. A. Drevon. 1988. Eicosapentaenoic acid inhibits cholesterol esterification in cultured parenchymal cells and isolated microsomes from rat liver. *J. Biol. Chem.* **263:** 8126–8132.

31. Lowry, O. H., N. J. Rosebrough, A. L. Farr, and R. J. Randall. 1951. Protein measurement with the Folin phenol reagent. *J. Biol. Chem.* **193:** 265–275.

32. Laemmli, U. K. 1970. Cleavage of structural proteins during the assembly of the head of bacteriophage T4. *Nature.* **227:** 680–685.

33. Tsai, A. C. 1975. Lipid peroxidation and glutathione peroxidase activity in the liver of cholesterol-fed rats. *J. Nutr.* **105:** 946–951.

34. Tsai, A. C., and N. S. C. Chen. 1979. Effect of cholesterol feeding on tissue glucose, insulin-degradation, serum lipids and serum lipoperoxide levels in rabbits. *J. Nutr.* **109:** 606–612.

35. Nagelkerke, J. F., K. P. Barto, and T. J. C. Van Berkel. 1983. In vivo and in vitro uptake and degradation of acetylated low density lipoprotein by rat liver endothelial, Kupffer and parenchymal cells. *J. Biol. Chem.* **258:** 12221–12227.

36. Blomhoff, R., C. A. Drevon, W. Eskild, P. Helgerud, K. R. Norum, and T. Berg. 1984. Clearance of acetyl low density lipoprotein by rat liver endothelial cells. *J. Biol. Chem.* **259:** 8898–8903.

37. Van Berkel, T. J. C., Y. B. De Rijke, and J. K. Kruijt. 1991. Different fate of oxidatively modified low density lipoprotein and acetylated low density lipoprotein in rats. *J. Biol. Chem.* **266:** 2282–2289.